STEM CELLS AND DEVELOPMENT
Volume 24, Number 13, 2015

DOI: 10.1089/scd.2014.0538

Reduction of Store-Operated Ca^{2+} Entry Correlates with Endothelial Progenitor Cell Dysfunction in Atherosclerotic Mice

Lian-You Wang, Ji-Hang Zhang, Jie Yu, Jie Yang, Meng-Yang Deng, Hua-Li Kang, and Lan Huang

The dysfunction of endothelial progenitor cells (EPCs) has been shown to prevent endothelial repair during the development of atherosclerosis (AS). Previous studies have revealed that store-operated calcium entry (SOCE) is an important factor in regulating EPC functions. However, whether this is also the mechanism in AS has not been elucidated. Therefore, we evaluated the role of SOCE in EPCs isolated from an atherosclerotic mouse model. Atheromatous plaques were more frequent in the aortas of $ApoE^{-/-}$ mice fed a high-fat diet for 16 weeks compared with controls, and the proliferative and migratory activities of atherosclerotic EPCs were significantly decreased. Accordingly, SOCE amplitude, as well as spontaneous or VEGF-induced Ca^{2+} oscillations, decreased in atherosclerotic EPCs. These results may be associated with the downregulated expression of Stim1, Orai1, and TRPC1, which are major mediators of SOCE. In addition, eNOS expression and phosphorylation at Ser^{1177}, which are critical regulators of EPC function, were markedly reduced in the atherosclerotic EPCs. The impairment of eNOS activity could also be induced by using an SOCE inhibitor or by Stim1 gene silencing, indicating a link between the activities of eNOS and SOCE in AS. Furthermore, decreased SOCE function inhibited EPC proliferation and migration in vitro. In conclusion, our results showed that the reduction of SOCE induced EPC dysfunction during AS, potentially through downregulation of store-operated calcium channel (SOCC) components and impaired eNOS activity. Approaches aimed at reestablishing SOCE activity may thus improve the function of EPCs during AS.

Introduction

Endothelial dysfunction is the process that initiates atherosclerosis (AS). Endothelial progenitor cells (EPCs) were once thought to be the seeds for vascular repair [1]; however, AS itself, as well as risk factors of AS, such as oxidized LDL (ox-LDL), diabetes mellitus, hypertension, and aging, interferes with EPC-mobilizing chemoattractant factor production and EPC survival/differentiation [2,3]. In addition, EPC dysfunction limits repair processes during endothelial injury. Therefore, rescuing EPC function is critical for repairing the endothelial lining. Unfortunately, ambiguity regarding the regulatory mechanisms underlying EPC functions has hindered the development of prevention and treatment strategies that target EPC dysfunction during AS.

Our prior studies have shown that store-operated calcium entry (SOCE) plays a critical role in the functions of EPCs and smooth muscle cells [4–6]. SOCE is mediated by store-operated calcium channels (SOCCs), which are activated in response to the depletion of intracellular Ca^{2+} stores. The key subunit of SOCC is Stim1, which was identified as a Ca^{2+} sensor in 2005. Stim1 senses changes in $[Ca^{2+}]_i$ within the ER and can migrate from the Ca^{2+} store to the plasma membrane to activate Ca^{2+} influx [7]. Another protein, Orai1, has been identified as a channel protein that mediates SOCE in multiple cell lineages, including immune cells [8], smooth muscle cells [9], and EPCs [10]. In addition, members of the TRPC family of nonselective cation channels, such as TRPC1, have been reported to be involved in SOCE in EPCs [5,10] and other cell types [11,12]. Despite previous research suggesting that SOCE participates in the regulation of EPC function in vitro, the role of SOCE in EPC dysfunction during AS remains unclear. In the current study, we obtained evidence that SOCE plays an essential role in the proliferative and migratory activities of EPCs during the process of AS.

Materials and Methods

Animal treatments and atherosclerotic lesion evaluation

All animal procedures were approved by the Experimental Animal Ethics Committee of the Third Military Medical University before performing the study and conformed to the

Institute of Cardiovascular Diseases of PLA, Xinqiao Hospital, Third Military Medical University, Chongqing, People's Republic of China.

regulations of the Guide for the Care and Use of Laboratory Animals of the US National Institutes of Health (NIH Publication No. 85-23, revised 1996).

Male ApoE$^{-/-}$ mice (6- to 8-week-old, C57BL/6J genetic background, Beijing University, Beijing, China) were randomly allocated into normal diet (ND) or high-fat diet (HFD, 21% fat, 0.15% cholesterol) groups. All animals were maintained at room temperature with a 12-h light/12-h dark cycle under specific pathogen-free conditions, with access to water ad libitum. At the end of 12 or 16 weeks of being fed the different diets, animals were anesthetized with an intramuscular injection of 100 mg/kg ketamine and 5 mg/kg xylazine. The atherosclerotic lesion burden along the luminal surface of the entire aorta was assessed using Oil red O staining as described previously [13].

Isolation and characterization of EPCs

EPCs were cultured and characterized as previously described [14]. The Materials and Methods and Results sections are described in detail in the Supplementary Data; Supplementary Data are available online at www.liebertpub.com/scd.

EPC numbers and proliferation assay

The number of EPCs was determined by directly counting the cells in six random high-power microscopic fields ($\times$400). The WST-8 assay was used to assess EPC proliferation. The cells were cultured in 96-well culture plates and underwent different pretreatments. Before the assay was performed, the cells were placed under serum-starved conditions for 6 h. Subsequently, 10 μL of WST-8 dye (Beyotime Institute of Technology) was added to each well, and the cells were incubated at 37°C for 4 h, after which the absorbance at 450 nm was determined using a microplate reader.

EPC migration assay

The migratory ability of the EPCs was evaluated using a modified Boyden chamber (Transwell; Corning) assay. In brief, the EPCs were treated with trypsin/EDTA, and then 4×10^4 EPCs were placed in the upper chamber in serum-free endothelial growth medium. The lower chamber was filled with conditional growth medium supplemented with VEGF (50 ng/mL). After incubation for 24 h, the membrane was washed using phosphate-buffered saline and fixed using 4% paraformaldehyde. The upper side of the membrane was wiped using a cotton ball. Then, the membrane was stained using a crystal violet solution. The migratory ability of the EPCs was evaluated by directly counting the cells in six random high-power ($\times$200) microscopic fields on the bottom of the membrane.

Gene silencing

A lentiviral vector carrying Stim1 shRNA was constructed by Gene Pharma. At 2 days after seeding mononuclear cells in wells, the lentiviral vector was added to the cells at a multiplicity of infection of 100. The transfection medium was removed 48 h later, and the cells were maintained in EGM-2 MV BulletKit medium (Lonza). The efficiency of the knockdown was confirmed using reverse transcription quantitative real-time PCR (RT-qPCR) and western blot analysis (Supplementary Fig. S2). The sequences of the oligonucleotides used in producing the shRNA targeting Stim1 mRNA are shown in the Supplementary Data.

Intracellular Ca^{2+} measurements

EPCs grown on glass-bottomed cell culture dishes were loaded with Fluo3 by incubating the cells for 40 min in 5 nM Fluo3-AM (Beyotime Institute of Technology). Then, Fluo3-AM was removed, and the cells were maintained in EGM-2 MV BulletKit medium for another 40 min before the measurements were made. The Ca^{2+} fluorescence was measured as previously described [15]. Briefly, the intracellular fluorescence intensity was measured at room temperature using a Leica confocal system (Leica TCS SP2). The fluorescence of 10–15 cells was measured simultaneously in every culture dish (excitation at 488 nm and emission at 530 nm). The region of interest was defined using the boundary of the individual cells. The laser intensity and photomultiplier gain were kept constant for all of the measurements. The free intracellular Ca^{2+} concentration ($[Ca^{2+}]_i$) was expressed as the fluorescence intensity F normalized to the baseline fluorescence value F0 (F/F0). Ca^{2+} influx was indicated as the $\Delta[Ca^{2+}]_i$ increase, which was calculated by subtracting F at the peak of the Ca^{2+} influx from the basal F0 value (Fmax-F0).

RT-qPCR analysis

Total RNA was isolated and purified using RNAiso Plus (TaKaRa). Single cDNAs were synthesized from RNA using a PrimeScript™ RT reagent kit (TaKaRa). RT-qPCR was performed in triplicate using 1 μg of cDNA and specific primers. SYBR® Premix Ex TaqTM II (Tli RNaseH Plus) (TaKaRa) was used according to the manufacturer's instruction, and RT-qPCR was performed using a StepOnePlus™ Real-time PCR System (Applied Biosystems). The conditions were as follows: initial denaturation at 95°C for 30 s, 40 cycles of denaturation at 95°C for 5 s, and then annealing for 30 s using the following annealing temperatures: Stim1 56°C; Orai1 60°C; and TRPC1 54°C. The relative mRNA levels were determined using the Δct method as described previously [16]. The specific primers are shown in the Supplementary Data.

Western immunoblot analysis

EPCs were lysed using a cell lysis buffer (M-PER; Pierce) supplemented with 0.5 mM PMSF and 2 mM sodium orthovanadate. Equal amounts of protein were separated using SDS-PAGE (10% polyacrylamide gel) and then electroblotted onto PVDF membranes for 120 min at 90 V. The membranes were blocked using a 5% nonfat milk solution in TBS containing 0.5% Tween 20 (for phosphorylated protein analysis, the membranes were blocked using a solution of 5% BSA in TBS containing 0.5% Tween 20). Then, the membranes were probed using antibodies directed against Stim1, eNOS, phospho-eNOS (Ser^{1177}), Akt, and phospho-Akt (Ser^{473}) (Cell Signaling Technology), as well as Orai1, TRPC1, and β-actin (Santa Cruz Technology). To determine the phospho-eNOS and phospho-Akt levels, the cells were stimulated using VEGF (10 ng/mL) for 60 min with or without PI 3-kinase inhibitor (LY-294002; Sigma-Aldrich). The labeled bands were detected using enhanced chemiluminescence

(Pierce). The densitometry signals were quantified using ImageQuant TL software.

Statistical analysis

The results are expressed as the mean ± SE for the data gathered from the cell biology experiments and as fold changes in expression compared with that of the controls (given as one-fold) for the data gathered from the molecular biology experiments. All statistical tests were conducted using SPSS 16.0 software. Student's *t*-tests were used for comparisons between groups. Values of $P < 0.05$ were considered statistically significant.

Results

EPC proliferative and migratory activities are decreased in atherosclerotic mice

In the present study, ApoE$^{-/-}$ mice fed a diet containing 21% fat and 0.15% cholesterol were used to create an AS model. As shown in Fig. 1A, more atherosclerotic lesions were observed in the aortas of the 12-week HFD ApoE$^{-/-}$ mice than in the aortas of the ND mice, and this effect was particularly marked in the 16-week HFD mice.

EPCs isolated from mouse bone marrow were cultured to analyze their proliferative and migratory abilities (the phenotype identification results are shown in the Supplementary Data). The proliferative activity of the EPCs was determined by both directly counting cells under a microscope and by performing the WST-8 assay. Accompanying the progression of AS, the numbers of EPCs derived from 12- and 16-week HFD mice (HFD-EPCs) decreased by 21% and 45% ($P < 0.05$), respectively, compared with the number of EPCs obtained from the ND mice (ND-EPCs) (Fig. 1B). Accordingly, the WST-8 assay revealed that the absorbance intensities for the 12-week and 16-week HFD-EPCs decreased by 41% and 64% ($P < 0.05$), respectively, compared with those of the ND-EPCs (Fig. 1C). The migratory activity of the EPCs was analyzed using a modified Boyden chamber. The results showed that the numbers of 12- and 16-week HFD-EPCs that reached the bottom of the membrane decreased by 34% and 42% ($P < 0.05$), respectively, compared with the number of ND-EPCs (Fig. 1D).

HFD-EPCs exhibit decreased SOCE activity

Because SOCE is critical in regulating the function of EPCs, we evaluated SOCE in EPCs obtained from ND, 12-week HFD, and 16-week HFD ApoE$^{-/-}$ mice. SOCE activation was monitored by subjecting the cells to a Ca^{2+} readdition protocol [17]. Thapsigargin (TG, 2 μM) was used to deplete the ER Ca^{2+} content in the absence of extracellular Ca^{2+} (0 Ca^{2+}), resulting in the first spike (Ca^{2+} release). A second spike was immediately observed following the readdition of Ca^{2+} to the bathing solution, representing Ca^{2+} entry through opened SOCCs (SOCE). There was no obvious Ca^{2+} release and only a miniscule amount of Ca^{2+} entry in the absence of TG stimulation. The amplitude of the TG-induced SOCE was significantly ($P < 0.05$) lower in HFD-EPCs than in ND-EPCs. The TG-induced Ca^{2+} release was also generally lower in HFD-EPCs, which may reflect decreased ER Ca^{2+} content (Fig. 2)

Orai1, Stim1, and TRPC1 expression is altered in HFD-EPCs

Stim1, Orai1, and TRPC1 are the major components of SOCCs and alterations in the levels of these proteins may

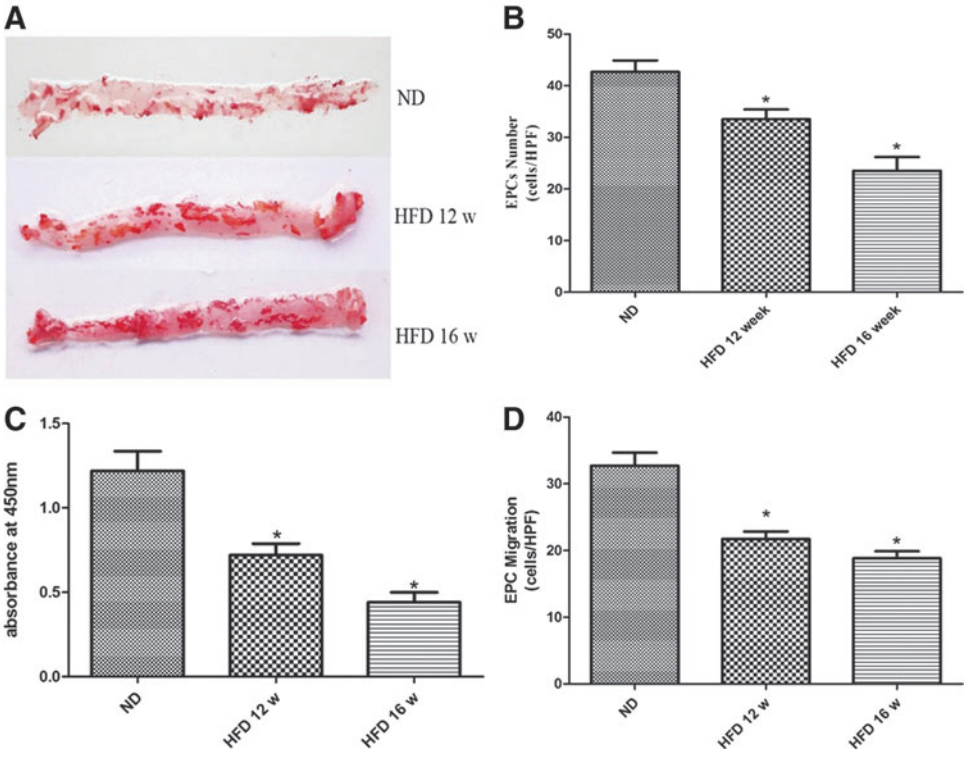

FIG. 1. Atherosclerosis (AS) reduced the proliferative and migratory activities of endothelial progenitor cells (EPCs). **(A)** Representative images showing lipid staining by Oil red O in the aortic trees obtained from normal diet (ND), 12-week high-fat diet (HFD), and 16-week HFD ApoE$^{-/-}$ mice. **(B)** The number of EPCs was counted under a microscope after 7 days in culture. The data are presented as the mean number of EPCs per high-power field (HPF) ± SE. **(C)** The proliferative activity of EPCs was assessed using a WST-8 assay. The data are presented as the mean absorbance at 450 nM ± SE. **(D)** EPC migration was evaluated by counting the number of EPCs on the bottom of a modified Boyden chamber membrane. The data are presented as the mean number of EPCs per HPF ± SE. $n = 5$, $^*P < 0.05$ versus ND-EPCs.

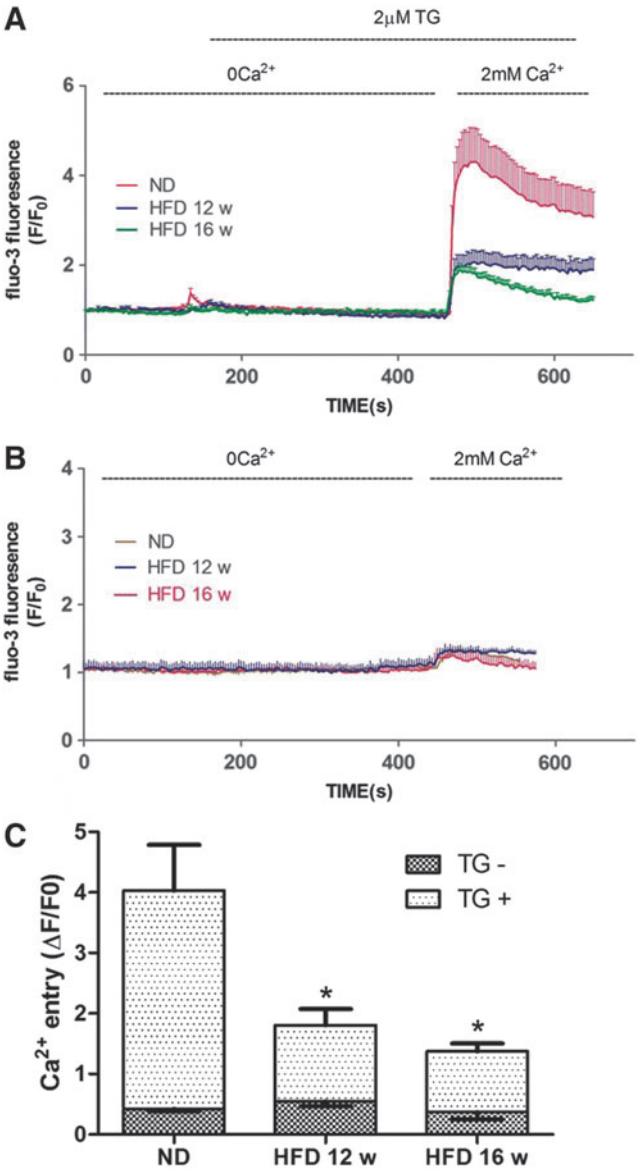

FIG. 2. Decreased store-operated calcium entry (SOCE) amplitude in HFD-EPCs. **(A)** Ca^{2+} was measured through confocal microscopy of cells stained with the fluorescent dye, Fluo3. During exposure to PSS without Ca^{2+}, Thapsigargin (TG) (2 μM) was used to deplete intracellular Ca^{2+} stores, after which Ca^{2+} (2 mM) was added back to the bathing medium, thereby eliciting a rise in $[Ca^{2+}]_i$ due to SOCE. The *red* (13 cells), *blue* (12 cells), and *green* (15 cells) traces depict representative time courses of $[Ca^{2+}]_i$ changes in EPCs isolated from ND, 12-, and 16-week HFD mice, respectively. **(B)** In the absence of TG stimulation, Ca^{2+} readdition resulted in only miniscule Ca^{2+} entry in EPCs. The *brown* (15 cells), *blue* (10 cells), and *red* (14 cells) traces depict representative time courses of $[Ca^{2+}]_i$ changes in EPCs isolated from ND, 12-, and 16-week HFD mice, respectively. **(C)** Quantification of Ca^{2+} entry amplitude. Cells in each group were harvested from three different mice. The data are presented as the mean ± SE. ND = 41, 12-week HFD = 35, 16-week HFD = 38, ND without TG = 38, 12-week HFD without TG = 30, 16-week HFD without TG = 35; $*P < 0.05$ versus ND-EPCs.

contribute to the magnitude of SOCE activity. In the present study, RT-qPCR analysis was used to investigate Stim1, Orai1, and TRPC1 mRNA levels. We found that in HFD-EPCs, Stim1, Orai1, and TRPC1 mRNA expression decreased with the progression of AS (Fig. 3A). Western blotting was then performed to probe Stim1, Orai1, and TRPC1 protein expression using affinity-purified antibodies. Densitometric analysis of the bands demonstrated that HFD-EPCs exhibited significantly lower levels of these proteins compared with ND-EPCs (Fig. 3B). Collectively, these results suggest that Orai1, Stim1, and TRPC1 expression levels were decreased in HFD-EPCs.

HFD-EPCs exhibit decreased Ca^{2+} oscillations

SOCE is an important component of Ca^{2+} oscillations, and recent data demonstrated that Ca^{2+} oscillations are involved in the proliferation and tubulogenesis of EPCs [18]. In this study, we observed little or no spontaneous Ca^{2+} oscillations in the HFD-EPCs during the testing period (30 min), and VEGF (used as a stimulus, at 10 ng/mL) elicited only a few detectable spikes of $[Ca^{2+}]_i$ in these cells, whereas ND-EPCs exposed to VEGF at the same dose produced obvious Ca^{2+} spikes (Fig. 4A, B). Furthermore, the amplitude of the spikes in HFD-EPCs was also lower than in ND-EPCs (Fig. 4A, C). Western blotting indicated no significant differences in the levels of VEGFR-2 expression in the HFD-EPCs and ND-EPCs, suggesting that the difference in their VEGF-induced Ca^{2+} oscillatory activities was independent of the level of VEGFR-2 (Supplementary Fig. S3).

SOCE activity correlates with eNOS activity in EPCs

As mentioned above, the SOCE amplitude and SOCE-dependent Ca^{2+} oscillations are involved in regulating EPC functions; however, how these processes are correlated remains unclear. eNOS is a key protein involved in the biological functions of EPCs [19], and eNOS activity is closely associated with Ca^{2+} activity. Thus, we investigated the relationship between the activities of SOCE and eNOS in EPCs. As shown in Figure 5, eNOS expression was downregulated in the HFD-EPCs. Accordingly, pharmacological and gene-silencing techniques were used to inhibit SOCE in ND-EPCs and both techniques reduced the levels of eNOS expression. These results suggest that SOCE is involved in eNOS expression. Next, VEGF (10 ng/mL) was used to stimulate EPCs to observe the role of SOCE in eNOS phosphorylation. As shown in Figure 6A, eNOS phosphorylation at Ser^{1177} was observed in EPCs as early as 5 min after VEGF stimulation, reaching a maximum response at the 30-min time point. Because several stimuli are known to activate eNOS through Akt-mediated phosphorylation, the role of Akt in eNOS phosphorylation was also evaluated in the present study. Akt phosphorylation at Ser^{473} was detected at 5 min poststimulation with VEGF (Fig. 6A), and treatment with a PI 3-kinase inhibitor inhibited the VEGF-induced phosphorylation of both eNOS and Akt (Supplementary Fig. S4). However, the levels of VEGF-induced eNOS and Akt phosphorylation were markedly lower in both HFD-EPCs and shStim1-ND-EPCs compared with those in ND-EPCs (Fig. 6B, C). These results suggest that reducing the level of SOCE affects eNOS phosphorylation (at least partly) through the PI3K/Akt pathway in EPCs.

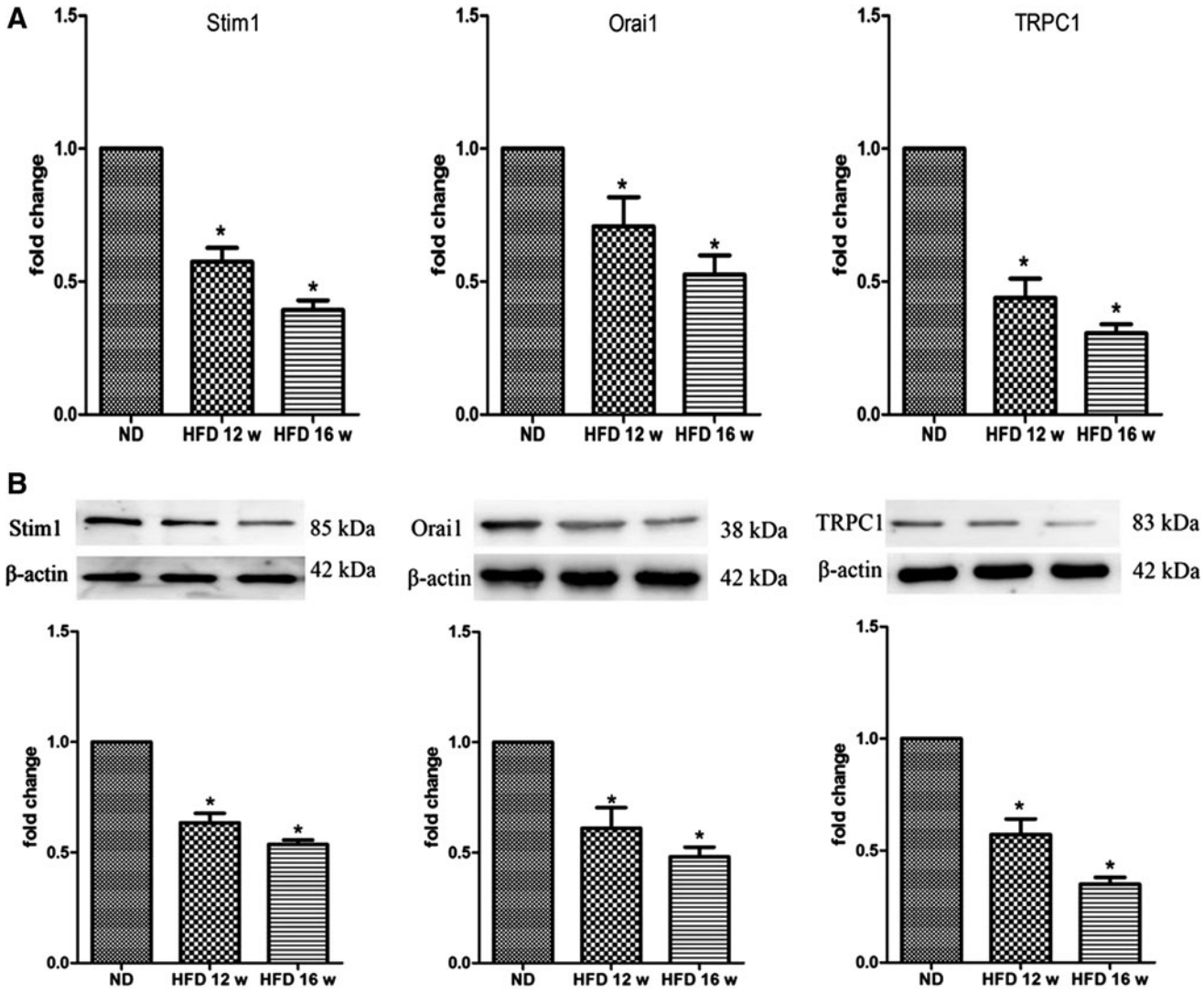

FIG. 3. Messenger RNA and protein expression of store-operated calcium channel (SOCC) components decreased in HFD-EPCs. **(A)** Stim1, Orai1, and TRPC1 mRNA levels were significantly reduced in HFD-EPCs compared with ND-EPCs by RT-qPCR. **(B)** Western blotting and densitometry analyses revealed significant reductions in the levels of Stim1, Orai1, and TRPC1 proteins in HFD-EPCs compared with ND-EPCs. The data are presented as the mean ± SE, $n = 3$; $^*P < 0.05$ versus ND-EPCs. RT-qPCR, reverse transcription quantitative real-time PCR.

SOCE inhibition reduces the proliferation and migration of EPCs

To assess whether inhibiting SOCE affects the proliferative and migratory activities of EPCs, we employed pharmacological and gene-silencing techniques to inhibit SOCE in ND-EPCs. Both 2-aminoethoxydiphenylborane (2-APB, 50 μM) and 1-(5-chloronaphthalene-1-sulfonyl)-1H-hexahydro-1,4-diazepine hydrochloride (ML-9, 50 μM), which have previously been reported as SOCE inhibitors, dramatically decreased ND-EPC proliferation and migration, as well as the SOCE amplitude induced by TG after 2 days of culture. Similarly, the genetic silencing of Stim1, which is the key mediator in gating SOCE, also resulted in markedly decreased SOCE amplitude and proliferative and migratory activities in ND-EPCs (Fig. 7). These data suggest that inhibiting SOCE decreases the proliferative and migratory activities of EPCs.

Discussion

In the present study, we identified a role for SOCE in regulating EPC function in an atherosclerotic mouse model. We found that the proliferative and migratory activities of EPCs decreased with the progression of AS. SOCE amplitude and Ca^{2+} oscillations were decreased in the EPCs isolated from atherosclerotic mice, which may correlate with the decreased expression of Orai1, Stim1, and TRPC1 in these cells. Furthermore, our data showed for the first time that the reduction of SOCE correlated with impaired eNOS activity in EPCs. Together, these novel findings suggest that decreased SOCE is correlated with EPC dysfunction during AS pathogenesis.

AS is generally recognized to be associated with reduced EPC numbers and with EPC dysfunction [2,3]. In the present study, we used an atherosclerotic mouse model to confirm that the proliferative and migratory activities of

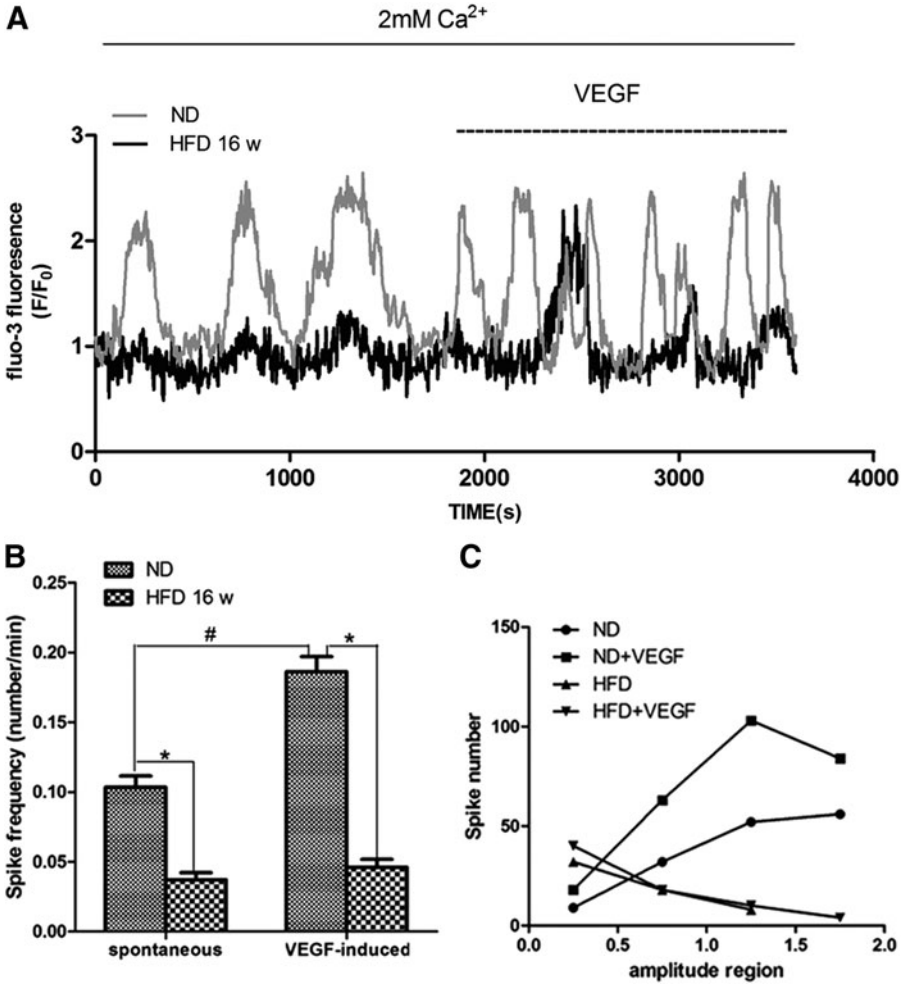

FIG. 4. Ca^{2+} oscillations were reduced in HFD-EPCs. **(A)** Representative image showing that spontaneous Ca^{2+} oscillations were minimal or absent in HFD-EPCs (0–1,800 s, *black*) compared with ND-EPCs (0–1,800 s, *gray*). VEGF (10 ng/mL) treatment elicited a burst of intracellular Ca^{2+} waves in ND-EPCs (1,800–3,600 s, *gray*), but elicited only a few intracellular Ca^{2+} waves in HFD-EPCs (1,800–3,600 s, *black*). **(B)** Comparison of spike frequency between ND-EPCs (48 cells) and HFD-EPCs (52 cells). $*,^{\#}P < 0.05$. **(C)** Comparison of amplitudes. Spike amplitudes were classified into four regions (0–0.5, 0.5–1, 1–1.5, 1.5–2). Spike numbers within each region were counted.

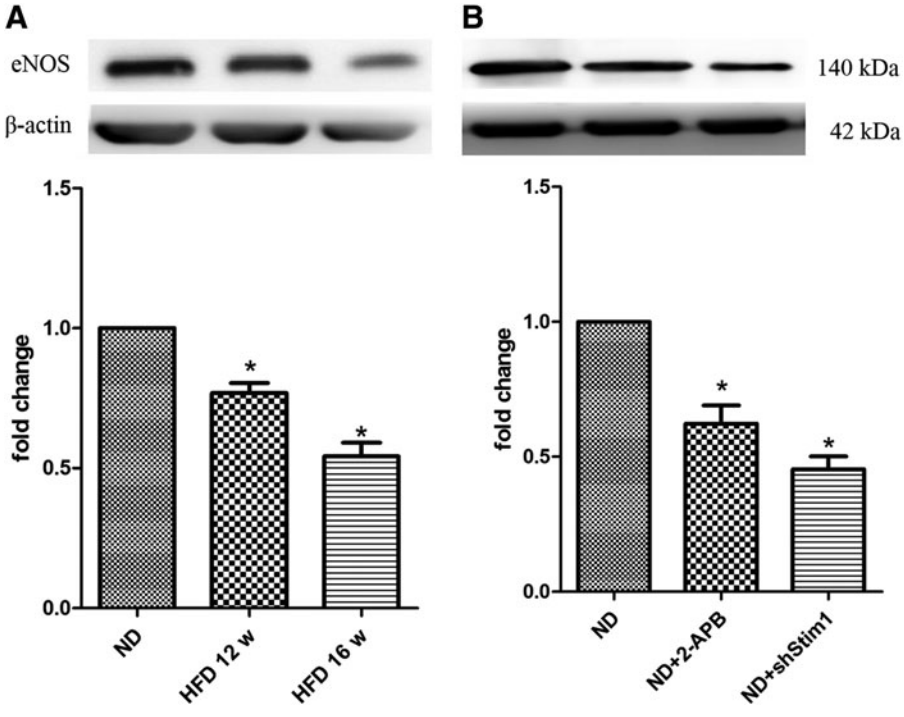

FIG. 5. eNOS expression was reduced in HFD-EPCs and in SOCE-inhibited EPCs. **(A)** Representative western blots for the detection of eNOS in EPCs that were isolated from ND, 12-week, and 16-week HFD $ApoE^{-/-}$ mice. **(B)** Representative western blots for the detection of eNOS in EPCs that were isolated from ND mice and that were treated with 2-APB or subjected to Stim1 gene silencing. $n = 3$, $*P < 0.05$ versus ND-EPCs.

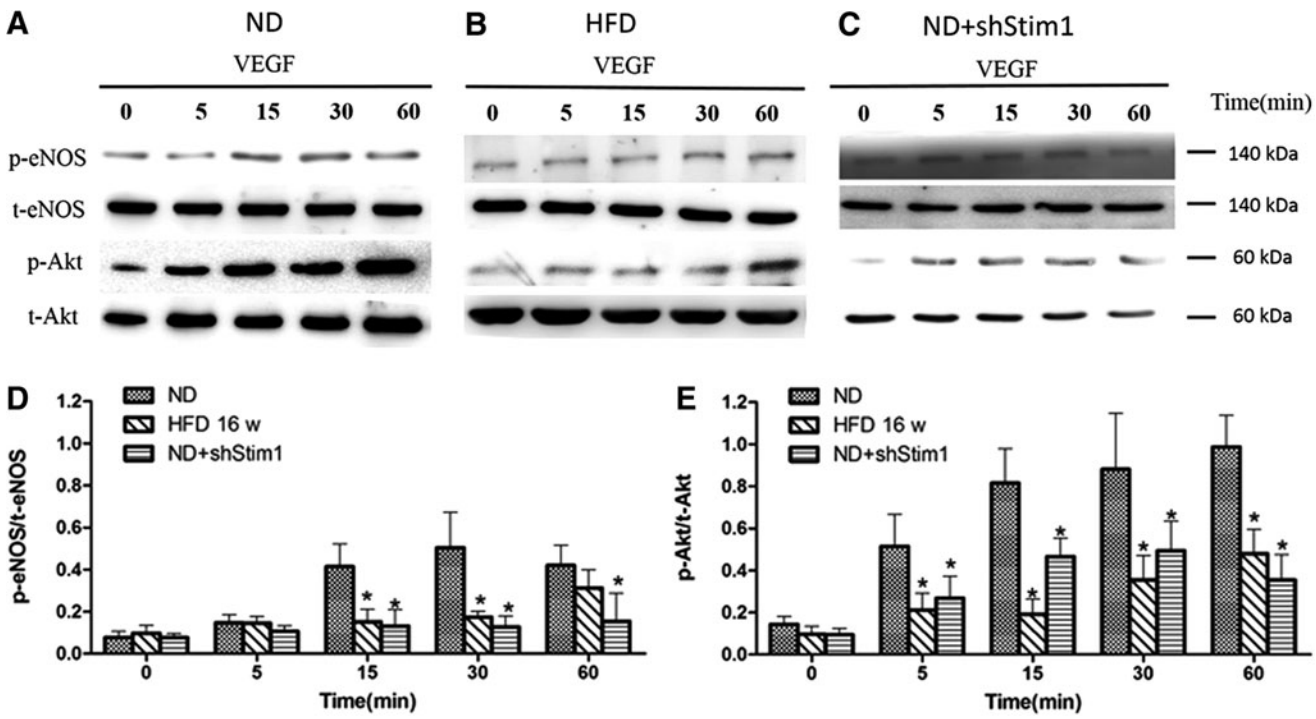

FIG. 6. VEGF-induced eNOS phosphorylation was reduced in HFD-EPCs and in SOCE-inhibited EPCs. **(A–C)** Representative western blots for the detection of phospho (p)-eNOS and p-Akt in ND-EPCs **(A)**, HFD-EPCs **(B)**, and ND-EPCs + shStim1 **(C)** stimulated with VEGF. **(D, E)** Quantitative analyses of VEGF-induced eNOS and Akt phosphorylation normalized to total eNOS or Akt, respectively. $n = 3$, $^*P < 0.05$ versus ND-EPCs.

EPCs decreased as AS progressed. However, it should be noted that most of the evidence regarding EPC dysfunction in AS is derived from patients, whereas in ApoE$^{-/-}$ mice, which are widely used AS animal models, the alteration of EPC function is still under debate. For example, Li et al. [33] found that in young ApoE$^{-/-}$ mice (fed aND), the number of EPCs and their migratory activities were greater than in WT mice. The progression of AS is associated with long-term exposure to oxidative stress [20] and inflammation [21], which markedly impair EPC function. Conversely, relatively short-term stimuli, such as hypercholesterolemia, may promote EPC function.

During the progression of AS, long-term oxidative stress and inflammation will affect a variety of physiological activities; in the present study, we focused on the activity of SOCE. As in previous studies [4], we used a specific sarcoplasmic/endoplasmic reticulum Ca^{2+}-ATPase (SERCA) inhibitor (TG) to induce SOCE and found that the SOCE amplitude was lower in HFD-EPCs. Not only did SOCE decrease but the amplitude of Ca^{2+} release from the ER also decreased in HFD-EPCs, which may have been due to decreased ER Ca^{2+} content. Indeed, the activation and amplitude of SOCE is not linearly correlated with the degree of ER Ca^{2+} content [22]. In addition, our data also showed that in HFD-EPCs, the expression of key components of SOCC (Stim1, Orai1, and TRPC1) was decreased. Under physiological conditions, store emptying is evoked by an increase in the levels of InsP3 or other Ca^{2+}-releasing signals [9], but in the present study, store emptying was induced by exposing cells to an SERCA inhibitor (TG), which prevents store refilling by P-type ATPases. In this condition, SOCE activation is independent of IP3R levels and is primarily determined by the activation of SOCCs. Thus, the results suggest that the reduced SOCE amplitude that accompanies the progression of AS is (at least partly) due to the impaired expression of SOCC subunits. However, the physiological activation of SOCE involves many regulatory mechanisms, such as the phosphorylation and dephosphorylation of Stim1 [23–25] and dynamic changes in the conformation of pore-forming proteins [26], which may also regulate SOCE in AS. The involvement of these processes needs to be illuminated in future studies.

As mentioned above, EPC dysfunction is accompanied by decreased SOCE in AS mice. Furthermore, we also demonstrated that inhibiting SOCE reduces the proliferative and migratory activities of EPCs in vitro, which was consistent with our previous findings [4] and was similar to the findings in HFD-EPCs. These results suggest that EPC dysfunction during AS is (at least partly) attributable to decreased SOCE.

Ca^{2+} oscillations are the primary form of Ca^{2+} signaling used to regulate a variety of cellular functions [27,28]. The generation of Ca^{2+} oscillations is dependent on Ca^{2+} release from Ca^{2+} stores [29] as well as on Ca^{2+} influx through membrane channels such as SOCCs [30]. For example, a previous study by Dragoni et al. [18] found that Ca^{2+} oscillations in EPCs can be partially blocked by either the absence of Ca^{2+} or the presence of a selective SOCE inhibitor. These findings concurred with our observations that Ca^{2+} oscillations are decreased in HFD-EPCs. Thus, we hypothesize that decreased SOCE in EPCs weakens Ca^{2+} oscillations during the development of AS, which consequently affects cellular functions. However, further studies are required to establish the exact relationship between SOCE, Ca^{2+} oscillations, and EPC function.

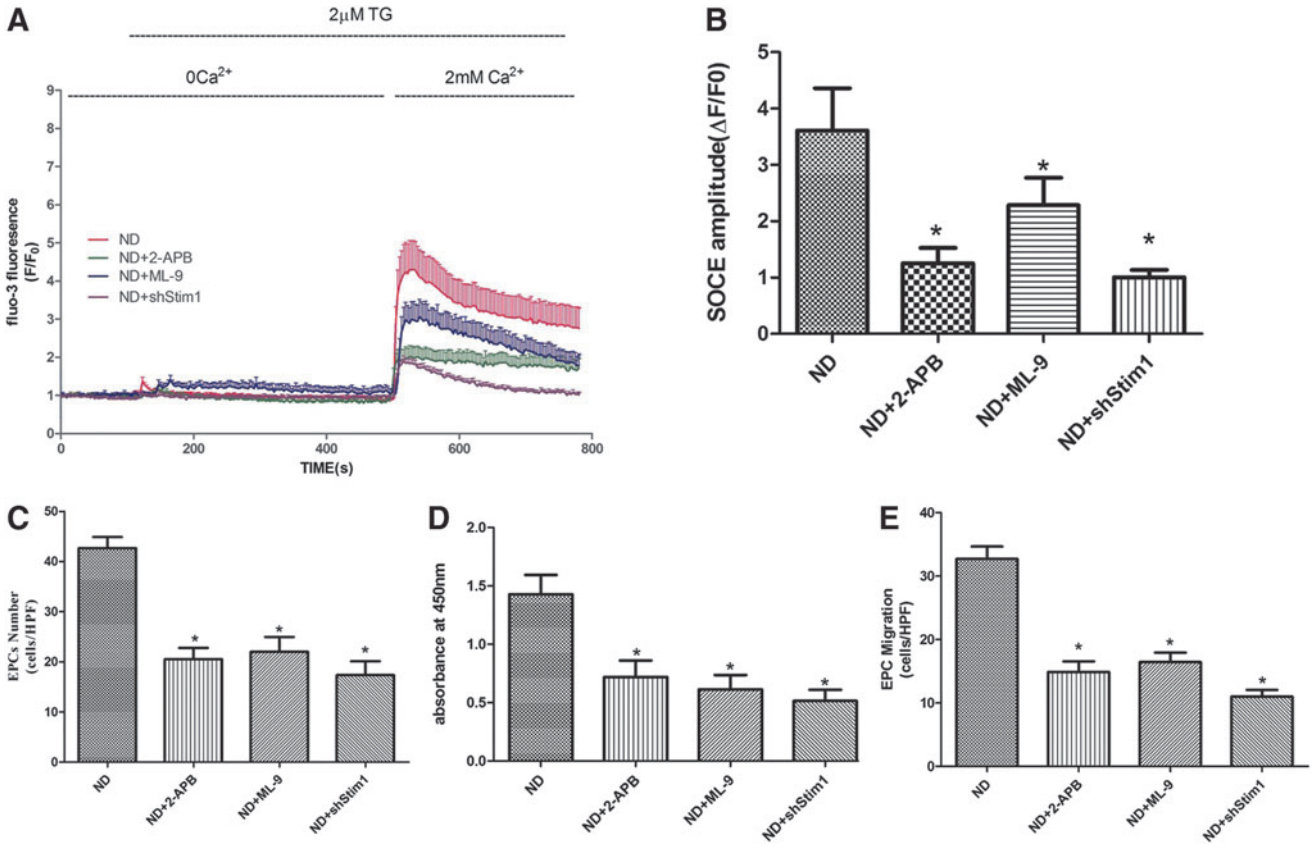

FIG. 7. SOCE inhibition reduced the proliferation and migration of EPCs. **(A)** Representative time courses of $[Ca^{2+}]_i$ changes showing that both specific inhibitors and shRNA-Stim1 inhibited SOCE in the ND-EPCs. ND = 13, ND + 2-APB = 15, ND + ML-9 = 12, ND + shStim1 = 13. **(B)** Quantification of TG-induced SOCE amplitudes. ND = 41, ND + 2-APB = 43, ND + ML-9 = 37, ND + shStim1 = 35. Cells in each group were harvested from three different mice. The data are presented as the mean ± SE; $*P < 0.05$ versus ND-EPCs. **(C)** The number of EPCs was counted under a microscope. **(D)** EPC proliferative activity was assessed by WST-8 assay. **(E)** EPC migration was evaluated by counting the number of EPCs on the bottom of a modified Boyden chamber membrane. **(C–E)** The data are presented as the mean ± SE, $n = 5$; $*P < 0.05$ versus ND-EPCs.

Interestingly, we found that eNOS activity is regulated by SOCE. eNOS is known to be a Ca^{2+}-dependent enzyme [31], and more importantly, NO production can be inhibited by the removal of Ca^{2+} from the extracellular fluid [32], indicating that Ca^{2+} influx may participate in the regulation of eNOS activity. Our results demonstrated that SOCE does in fact participate in VEGF-induced eNOS phosphorylation in EPCs. Furthermore, the expression of eNOS in EPCs was also found to be regulated by SOCE. These results provide direct evidence of a clear link between SOCE and eNOS activity.

Taken together, the results of the present study demonstrate for the first time that altered SOCE is closely associated with EPC dysfunction in atherosclerotic mice. This effect may occur through the following mechanisms: (1) the downregulation of SOCC components, followed by decreased Ca^{2+} oscillations, which play an important role in regulating EPC functions; and/or (2) decreased eNOS expression and phosphorylation. Hence, therapeutic approaches aimed at regulating SOCE may be useful in limiting the extent of EPC dysfunction.

Acknowledgments

This study was supported by the National Natural Science Foundation of China (grant 81370211). The authors gratefully acknowledge Prof. J.H.Z. for critical comments on manuscript editing and review.

Author Disclosure Statement

No conflicts of interest exist.

References

1. Lamping K. (2007). Endothelial progenitor cells: sowing the seeds for vascular repair. Circ Res 100:1243–1245.
2. Hill JM, G Zalos, JP Halcox, WH Schenke, MA Waclawiw, AA Quyyumi and T Finkel. (2003). Circulating endothelial progenitor cells, vascular function, and cardiovascular risk. N Engl J Med 348:593–600.
3. Du F, J Zhou, R Gong, X Huang, M Pansuria, A Virtue, X Li, H Wang and XF Yang. (2012). Endothelial progenitor cells in atherosclerosis. Front Biosci (Landmark Ed) 17: 2327–2349.
4. Kuang CY, Y Yu, RW Guo, DH Qian, K Wang, MY Den, YK Shi and L Huang. (2010). Silencing stromal interaction molecule 1 by RNA interference inhibits the proliferation and migration of endothelial progenitor cells. Biochem Biophys Res Commun 398:315–320.

5. Kuang CY, Y Yu, K Wang, DH Qian, MY Den and L Huang. (2012). Knockdown of transient receptor potential canonical-1 reduces the proliferation and migration of endothelial progenitor cells. Stem Cells Dev 21:487–496.
6. Guo RW, H Wang, P Gao, MQ Li, CY Zeng, Y Yu, JF Chen, MB Song, YK Shi and L Huang. (2009). An essential role for stromal interaction molecule 1 in neointima formation following arterial injury. Cardiovasc Res 81:660–668.
7. Zhang SL, Y Yu, J Roos, JA Kozak, TJ Deerinck, MH Ellisman, KA Stauderman and MD Cahalan. (2005). STIM1 is a Ca2+ sensor that activates CRAC channels and migrates from the Ca2+ store to the plasma membrane. Nature 437:902–905.
8. Feske S, Y Gwack, M Prakriya, S Srikanth, SH Puppel, B Tanasa, PG Hogan, RS Lewis, M Daly and A Rao. (2006). A mutation in Orai1 causes immune deficiency by abrogating CRAC channel function. Nature 441:179–185.
9. Parekh AB and JW Putney, Jr. (2005). Store-operated calcium channels. Physiol Rev 85:757–810.
10. Sanchez-Hernandez Y, U Laforenza, E Bonetti, J Fontana, S Dragoni, M Russo, JE Avelino-Cruz, S Schinelli, D Testa, et al. (2010). Store-operated Ca(2+) entry is expressed in human endothelial progenitor cells. Stem Cells Dev 19:1967–1981.
11. Liu X, W Wang, BB Singh, T Lockwich, J Jadlowiec, B O'Connell, R Wellner, MX Zhu and IS Ambudkar. (2000). Trp1, a candidate protein for the store-operated Ca(2+) influx mechanism in salivary gland cells. J Biol Chem 275:3403–3411.
12. Xu SZ and DJ Beech. (2001). TrpC1 is a membrane-spanning subunit of store-operated Ca(2+) channels in native vascular smooth muscle cells. Circ Res 88:84–87.
13. Heller EA, E Liu, AM Tager, Q Yuan, AY Lin, N Ahluwalia, K Jones, SL Koehn, VM Lok, et al. (2006). Chemokine CXCL10 promotes atherogenesis by modulating the local balance of effector and regulatory T cells. Circulation 113:2301–2312.
14. Asahara T, T Murohara, A Sullivan, M Silver, R van der Zee, T Li, B Witzenbichler, G Schatteman and JM Isner. (1997). Isolation of putative progenitor endothelial cells for angiogenesis. Science 275:964–967.
15. Zou JJ, YD Gao, S Geng and J Yang. (2011). Role of STIM1/Orai1-mediated store-operated Ca(2)(+) entry in airway smooth muscle cell proliferation. J Appl Physiol (1985) 110:1256–1263.
16. Pfaffl MW. (2001). A new mathematical model for relative quantification in real-time RT-PCR. Nucleic Acids Res 29:e45.
17. Bird GS, WI DeHaven, JT Smyth and JW Putney, Jr. (2008). Methods for studying store-operated calcium entry. Methods 46:204–212.
18. Dragoni S, U Laforenza, E Bonetti, F Lodola, C Bottino, R Berra-Romani, G Carlo Bongio, MP Cinelli, G Guerra, et al. (2011). Vascular endothelial growth factor stimulates endothelial colony forming cells proliferation and tubulogenesis by inducing oscillations in intracellular Ca^{2+} concentration. Stem Cells 29:1898–1907.
19. Everaert BR, EM Van Craenenbroeck, VY Hoymans, SE Haine, L Van Nassauw, VM Conraads, JP Timmermans and CJ Vrints. (2010). Current perspective of pathophysiological and interventional effects on endothelial progenitor cell biology: focus on PI3K/AKT/eNOS pathway. Int J Cardiol 144:350–366.
20. Schnabel R and S Blankenberg. (2007). Oxidative stress in cardiovascular disease: successful translation from bench to bedside? Circulation 116:1338–1340.
21. Willerson JT and PM Ridker. (2004). Inflammation as a cardiovascular risk factor. Circulation 109:II2–II10.
22. Palty R, A Raveh, I Kaminsky, R Meller and E Reuveny. (2012). SARAF inactivates the store operated calcium entry machinery to prevent excess calcium refilling. Cell 149: 425–438.
23. Sundivakkam PC, V Natarajan, AB Malik and C Tiruppathi. (2013). Store-operated Ca2+ entry (SOCE) induced by protease-activated receptor-1 mediates STIM1 protein phosphorylation to inhibit SOCE in endothelial cells through AMP-activated protein kinase and p38beta mitogen-activated protein kinase. J Biol Chem 288:17030–17041.
24. Lee HJ, GU Bae, YE Leem, HK Choi, TM Kang, H Cho, ST Kim and JS Kang. (2012). Phosphorylation of Stim1 at serine 575 via netrin-2/Cdo-activated ERK1/2 is critical for the promyogenic function of Stim1. Mol Biol Cell 23:1376–1387.
25. Pozo-Guisado E, V Casas-Rua, P Tomas-Martin, AM Lopez-Guerrero, A Alvarez-Barrientos and FJ Martin-Romero. (2013). Phosphorylation of STIM1 at ERK1/2 target sites regulates interaction with the microtubule plus-end binding protein EB1. J Cell Sci 126:3170–3180.
26. Ong HL, KT Cheng, X Liu, BC Bandyopadhyay, BC Paria, J Soboloff, B Pani, Y Gwack, S Srikanth, et al. (2007). Dynamic assembly of TRPC1-STIM1-Orai1 ternary complex is involved in store-operated calcium influx. Evidence for similarities in store-operated and calcium release-activated calcium channel components. J Biol Chem 282:9105–9116.
27. Parekh AB. (2011). Decoding cytosolic Ca2+ oscillations. Trends Biochem Sci 36:78–87.
28. Dupont G, L Combettes, GS Bird and JW Putney. (2011). Calcium oscillations. Cold Spring Harb Perspect Biol 3:pii: a004226.
29. Berridge MJ. (2007). Inositol trisphosphate and calcium oscillations. Biochem Soc Symp 1–7.
30. Putney JW and GS Bird. (2008). Cytoplasmic calcium oscillations and store-operated calcium influx. J Physiol 586: 3055–3059.
31. Busse R and A Mulsch. (1990). Calcium-dependent nitric oxide synthesis in endothelial cytosol is mediated by calmodulin. FEBS Lett 265:133–136.
32. Luckhoff A, U Pohl, A Mulsch and R Busse. (1988). Differential role of extra- and intracellular calcium in the release of EDRF and prostacyclin from cultured endothelial cells. Br J Pharmacol 95:189–196.
33. Ii M, K Takeshita, K Ibusuki, C Luedemann, A Wecker, E Eaton, T Thorne, T Asahara, JK Liao and DW Losordo. (2010). Notch signaling regulates endothelial progenitor cell activity during recovery from arterial injury in hypercholesterolemic mice. Circulation 121:1104–1112.

Address correspondence to:
Dr. Lan Huang
Institute of Cardiovascular Diseases of PLA
Xinqiao Hospital
Third Military Medical University
Chongqing 400037
People's Republic of China

E-mail: huanglan260@126.com

Received for publication November 16, 2014
Accepted after revision February 18, 2015
Prepublished on Liebert Instant Online March 9, 2015